Title	Theoretical study of the rate constants for the hydrogen atom abstraction reactions of esters with •OH radicals
Author(s)	Mendes, Jorge; Zhou, Chong-Wen; Curran, Henry J.
Publication Date	2014-05-30
Publication Information	Mendes, J,Zhou, CW,Curran, HJ (2014) 'Theoretical study of the rate constants for the hydrogen atom abstraction reactions of esters with •OH radicals'. Journal Of Physical Chemistry A, 118 :4889-4899.
Publisher	American Chemical Society
Link to publisher's version	http://dx.doi.org/10.1021/jp5029596
Item record	http://hdl.handle.net/10379/6148
DOI	http://dx.doi.org/10.1021/jp5029596

Theoretical Study Of The Rate Constants For The Hydrogen Atom Abstraction Reactions Of Esters With ȮH Radicals

Jorge Mendes, Chong-Wen Zhou,* and Henry J. Curran

Combustion Chemistry Centre, National University of Ireland, Galway, Ireland.

E-mail: chongwen.zhou@nuigalway.ie

*To whom correspondence should be addressed

Abstract

A systematic investigation of the rate constants for the hydrogen atom abstraction reactions by hydroxyl radicals on esters has been performed. The geometry optimizations and frequency calculations have been obtained using the second order Møller-Plesset method with the 6-311G(d,p) basis set. The same method has also been used in order to determine the dihedral angle potential for each individual hindered rotor in each reactant and transition state. Intrinsic reaction coordinate calculations have been used in order to connect each transition state to the corresponding local minimum. For the reactions of methyl ethanoate with an $\dot{O}H$ radical, the relative electronic energies have been calculated using the G3 and the CCSD(T)/cc-pV*X*Z method (where X = D, T and Q) which were extrapolated to the complete basis set limit (CBS). The electronic energies obtained using the G3 method were then benchmarked against the CBS results and were found to be within 1 kcal mol^{-1} of one another. Rate constants have been determined at the high-pressure limit by conventional transition state theory, with a correction for asymmetric Eckart tunneling, using the energies obtained with the G3 method. We report the individual, average and total rate constants in the temperature range from 500 to 2200 K. Our reported total rate constant results were compared to experimental data obtained by Lam *et al.* and our calculated results are within a factor of 2 for methyl ethanoate and between 40–50% for methyl propanoate and methyl butanoate.

Keywords

ab-initio, hydroxyl radical, oxygenated fuels, theoretical, kinetics

Introduction

Due to the depletion of fossil derived fuels and the environmental impact these fuels have on the atmosphere, interest in biofuels has been increasing.[1] Esters can be obtained from several types of oil including soybean in the United States and rapeseed in Europe[2] and they are a component of biodiesel. They are typically made of a long $(16-18)$ carbon atom chains which require very large detailed chemical kinetic models[3] to describe their oxidation. Despite this complexity, however, there has been an effort in understanding the reactivity of such large molecules by studying smaller molecules, such as methyl formate and methyl butanoate.[2]

Recently, Lam *et al.* experimentally measured the rate constants for the reactions of hydroxyl radicals with methyl formate, methyl ethanoate, methyl propanoate and methyl butanoate using a shock-tube equipped with UV laser absorption.[2] Dooley *et al.* studied the autoignition behavior of methyl butanoate and developed a detailed chemical kinetic model based on experiments in a shock-tube and in a rapid compression machine and other literature data.[4] Fisher *et al.* developed a chemical kinetic model for methyl formate and methyl butanoate combustion.[5] Hakka *et al.* developed a mechanism to describe the oxidation of methyl and ethyl butanoates.[6] Diévart *et al.* studied the chemical kinetic characteristics of small methyl esters.[7] Westbrook *et al.* developed a chemical kinetic mechanism for methyl formate, methyl ethanoate, ethyl formate and ethyl ethanoate.[3]

In the temperature range 500 to 2000 K, abstraction reactions by $\dot{\text{O}}\text{H}$ radicals on stable species are very important. To our knowledge, accurate high level *ab initio* and rate constant calculations of the title reactions have not previously been performed. Herein, we detail a systematic study of these reactions on several esters: methyl (ethanoate, propanoate, butanoate and isobutyrate) and ethyl, propyl and isopropyl (ethanoate). In our previous work we have studied the influence of the RC=OOR′ group on several esters when $\text{H}\dot{\text{O}}_2$ radicals abstract a 1°, 2° or 3° hydrogen atom.[1] In this work we investigate the influence of the same functional group on similar reactions with $\dot{\text{O}}\text{H}$ radicals. As with our previous works on ketones,[8–10] esters,[1] ethers[11,12] and alcohols,[13,14] a similar stepwise mechanism was determined where the formation of complexes occurs in the entrance and exit channels. In our previous work on ketones + $\dot{\text{O}}\text{H}$ radicals,[10] two conformers

(gauche and trans) with similar chemical properties are formed at the α and β positions relative to the RC=OR′ group. In esters + $\dot{H}O_2$ radicals[1] we have reported that for the methyl pentanoate reactant, the energy for the rotation of the α'–β' and β'–γ' hindered rotors is 4.5 and 5.7 kcal mol^{-1}, respectively. We have also reported that the relative electronic energy of the gauche reactant conformer is 4 kcal mol^{-1} higher than that of the trans reactant conformer. Therefore, as in our previous works,[1,8,9,12] only the trans reactant conformers are considered herein.

Methodology

The second order Møller-Plesset (MP2) method and the 6-311G(d,p) basis set were used in the geometry optimizations and frequency calculations of all of the species using Gaussian-09.[15] The same method was also used to determine the potential energy surface scans for the individual hindered rotors associated with each reactant and transition state. Intrinsic reaction coordinate calculations have been used in order to connect each transition state to the corresponding local minimum. For the hydrogen atom abstraction reactions of methyl ethanoate + ȮH radicals, the relative electronic energies have been calculated with the G3 method and at the CCSD(T)/cc-pVXZ level of theory (where X = D, T and Q) which were extrapolated to the complete basis set (CBS) limit.[16] Relative electronic energies, in kcal mol^{-1}, were obtained by the G3 method and are within 1 kcal mol^{-1} of the extrapolated CBS limit energies. As the CCSD(T)/CBS method is computationally more expensive for the larger molecules in this study, the G3 method has been used in the determination of the relative electronic energies of all of the species. Visualization as well as the determination of geometrical parameters have been performed with ChemCraft.[17]

Conventional transition state theory[18] with an asymmetric Eckart tunneling correction,[19] as implemented in Variflex v2.02m,[20] has been used in order to calculate the high-pressure limit rate constants in this work, in the temperature range from 500 to 2200 K:

$$k^{\mathrm{TST}}(T) = \kappa \frac{\mathrm{k}_B T}{\mathrm{h}} \frac{\mathrm{Q}^{\ddagger}(T)}{\mathrm{Q}_A(T)\mathrm{Q}_B(T)} \exp\left(-\frac{\mathrm{E}^{\ddagger}}{\mathrm{k}_B T}\right) \quad (1)$$

Where $k^{\mathrm{TST}}(T)$ is the rate constant at temperature T; κ is the asymmetric Eckart tunneling factor; k_B is the Boltzmann constant; h is the Planck constant; $Q^{\ddagger}(T)$ is the partition function for the transition state; $Q_A(T)$ and $Q_B(T)$ are the partition functions for the reactants and $E^{\ddagger}$ is the calculated electronic energy barrier height. Each partition function is evaluated with respect to the zero-point levels of reactants and transition states and are the product of translational (Q_{trans}), vibrational (Q_{vib}), external rotational (Q_{rot}), torsional (Q_{tor}) and electronic (Q_{el}) partition functions ($Q = Q_{trans} \times Q_{vib} \times Q_{rot} \times Q_{tor} \times Q_{el}$).

Georgievskii *et al.*[21] have studied the kinetics of C_2H_6 + CN abstraction reactions. Their theoretical calculations are based on two distinct transition state regimes comprising an outer and an inner transition state. At low temperatures ($T < 200$ K) they have found that the rate determining step is the formation of the van der Waals complex (outer transition state). However, at higher temperatures ($T > 200$ K) they determined that overcoming the barrier of the saddle point (inner transition state) is the rate determining step and a two transition state model over-estimates the rate constants. Therefore, at temperatures above 200 K a single inner transition state description can be used for estimating the rate constants. In this work, we estimate rate constants over the temperature range from 500 K to 2200 K and based on Georgievskii *et al.* conclusions, the single inner transition state is the rate determining step. Therefore, we disregard the effect of the outer transition state.

Potential Energy Surface

Figure 1 and Table 1 are given in order to define the nomenclature used in this work. The geometries of the esters, optimized at the MP2/6-311G(d,p) level of theory, are shown in Figures 2(a)–2(g). Table S1 in the Supporting Information (SI) details all of the energies calculated for methyl ethanoate + $\dot{\mathrm{O}}$H radicals at the CCSD(T)/cc-pVXZ (X = D, T, Q) and CCSD(T)/CBS levels of theory in kcal mol^{-1}. The geometries and frequencies for the reactants and transitions states in this work are given in Table S2 in the SI.

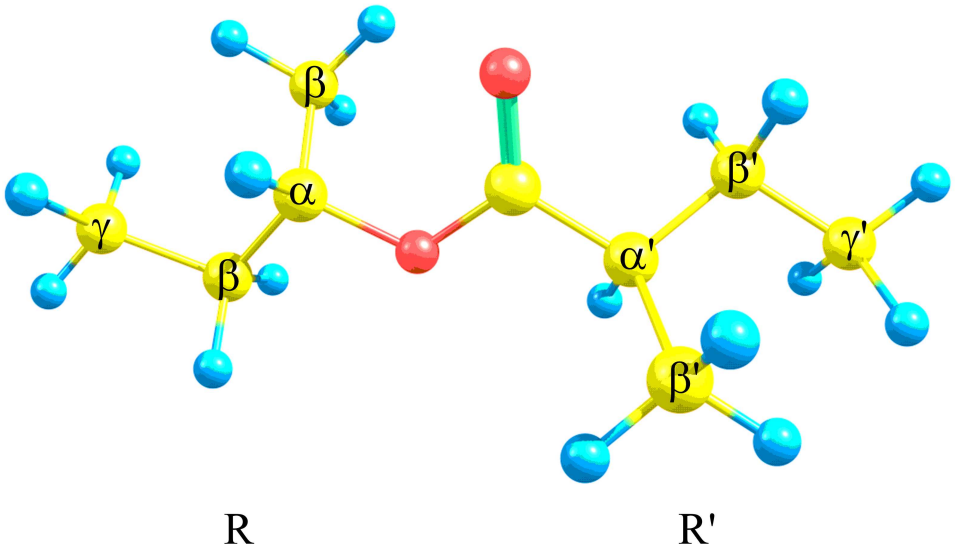

Figure 1: Labels in use in this work.

Table 1: Electronic energies (in kcal mol^{-1}) of the transition states relative to the reactants for esters + ȮH radicals in this work, detailing the different types of hydrogen atoms present.

		γ'	β'	α'	α	β	γ
(a)	$CH_3C{=}OOCH_3$ (ME)			3.43 (1°)	0.69 (1°)		
(b)	$CH_3CH_2C{=}OOCH_3$ (MP)		0.64 (1°)	0.65 (2°)	0.54 (1°)		
(c)	$CH_3(CH_2)_2C{=}OOCH_3$ (MB)	2.76 (1°)	−1.88 (2°)	0.21 (2°)	0.48 (1°)		
(d)	$(CH_3)_2CHC{=}OOCH_3$ (MiB)		0.67 (1°)	−1.49 (3°)	0.30 (1°)		
(e)	$CH_3C{=}OOCH_2CH_3$ (EE)			3.26 (1°)	−1.55 (2°)	2.48 (1°)	
(f)	$CH_3C{=}OO(CH_2)_2CH_3$ (PE)			3.23 (1°)	−2.07 (2°)	−0.10 (2°)	2.97 (1°)
(g)	$CH_3C{=}OOCH(CH_3)_2$ (iPE)			3.12 (1°)	−2.72 (3°)	1.92 (1°)	

Figure 4 shows the potential energy surface (PES) for the reactions of ME + ȮH radicals obtained with the G3 method and at CCSD(T)/CBS level of theory (in parentheses), in kcal mol^{-1}. Figure 5–10 show the PES obtained with the G3 method for the reactions of an ȮH radical when abstracting a hydrogen atom from MP (Figure 5), MB (Figure 6), MiB (Figure 7), EE (Figure 8), PE (Figure 9) and iPE (Figure 10), in kcal mol^{-1}. Table 1 details the electronic energies relative to the reactants of each transition state at each position relative to the RC=OOR′ group, and the type of hydrogen atom present.

As in our previous studies,[1,8–10,12] we determined that complexes are formed in both the entrance and exit channels which will narrow the tunneling barrier, accelerating the tunneling effect

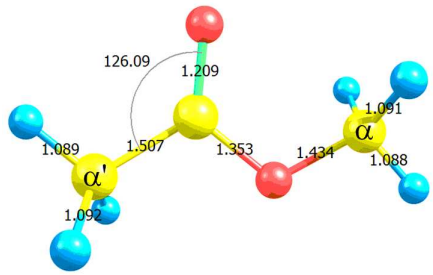

(a) Methyl ethanoate (ME)

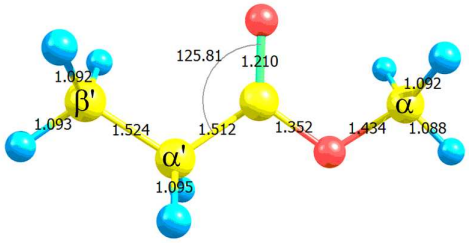

(b) Methyl propanoate (MP)

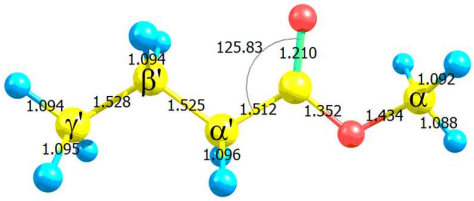

(c) Methyl butanoate (MB)

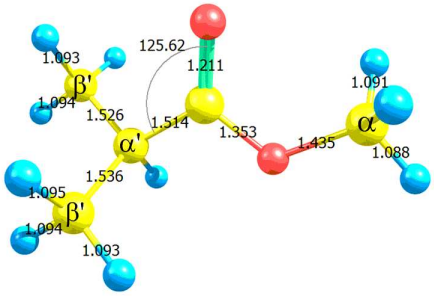

(d) Methyl isobutyrate (MiB)

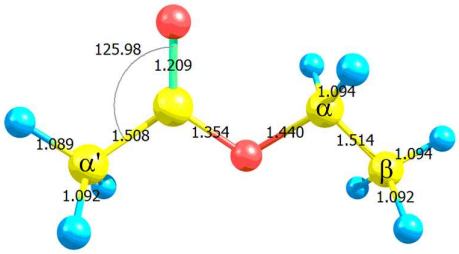

(e) Ethyl ethanoate (EE)

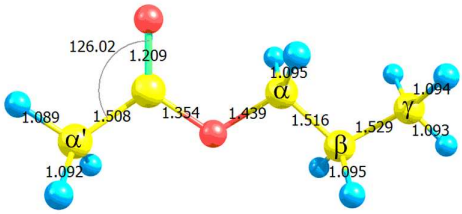

(f) Propyl ethanoate (PE)

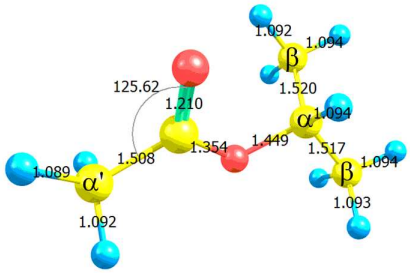

(g) Isopropyl ethanoate (iPE)

Figure 2: Optimized geometries of the esters in this work at MP2/6-311G(d,p) level of theory, detailing the different labels we use.

and, consequently, the rate constants. In order to quantify this influence of the reactant and product complexes in our results, we have calculated the rate constants for abstraction of a hydrogen atom at the α' position of ME and the comparison is shown in Figure 3. We observe that when considering the formation of these complexes, the rate constants increase by 68% at 500 K. Reactant complexes (RC) have relative energies in the range from -5.63 to -3.56 kcal mol^{-1} and product complexes (PC) range from -30.84 to -17.65 kcal mol^{-1}. The formation of reactant complexes is not observed when abstracting a hydrogen atom at the γ' and γ positions due to the distance between the ȮH radical and the RC=OOR′ group. Apart from these reaction channels, most of the reactant and product complexes found form a hydrogen bond between the hydrogen atom of the hydroxyl radical and one of the oxygen atoms of the RC=OOR′ group. The same behavior was observed with the transition states where, apart from abstraction at the γ' and γ positions, a hydrogen bond is formed between the ȮH radical and the RC=OOR′ group for all of the transition states. We have treated all low-frequency torsional modes as hindered rotors.

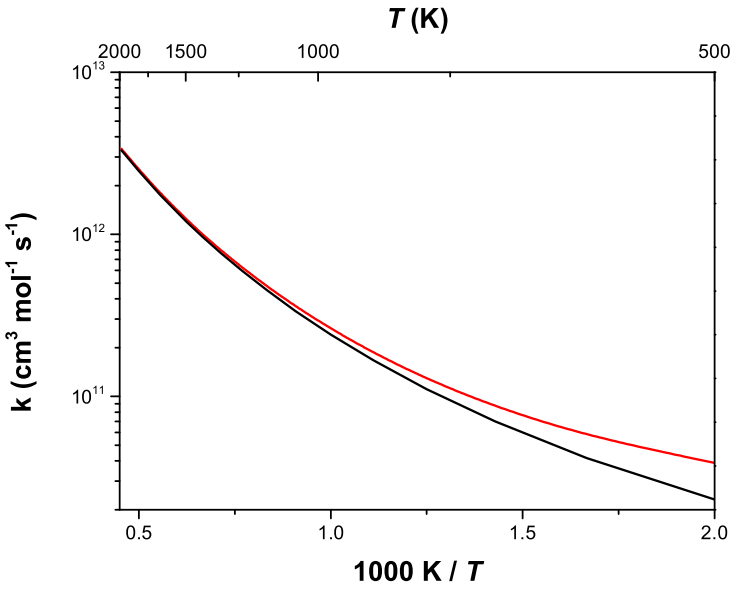

Figure 3: Rate constants for ME with (red line) and without (black line) the inclusion of the reactant and product complexes.

Hydrogen atom abstraction occurs in a similar fashion at each position of the esters in this work

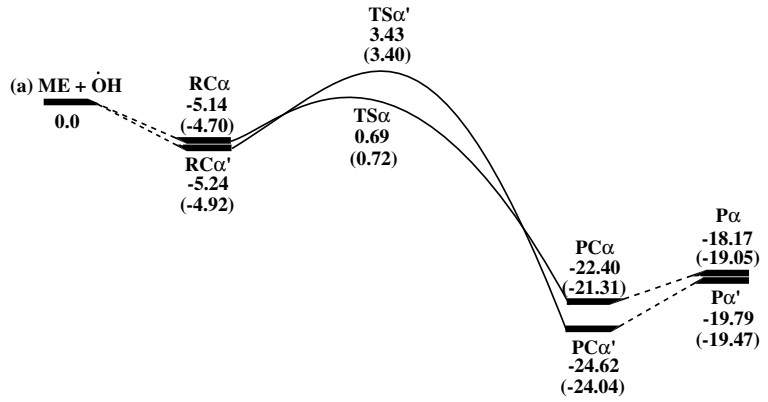

Figure 4: Potential Energy Surface of the reactions of ME + ȮH radicals calculated with the G3 method and CCSD(T)/CBS (in parentheses), in kcal mol^{-1}.

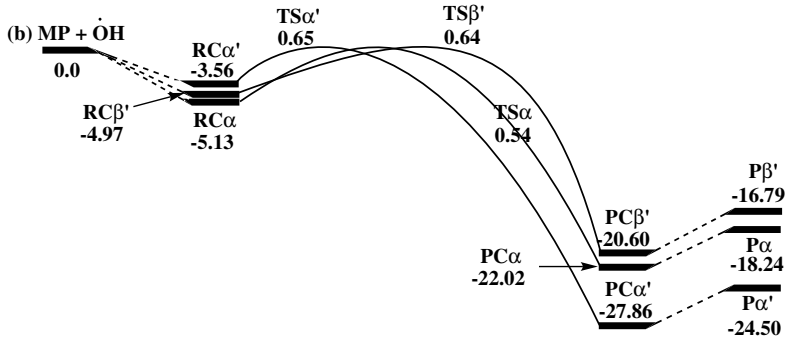

Figure 5: Potential Energy Surface of the reactions of MP + ȮH radicals calculated with the G3 method, in kcal mol^{-1}.

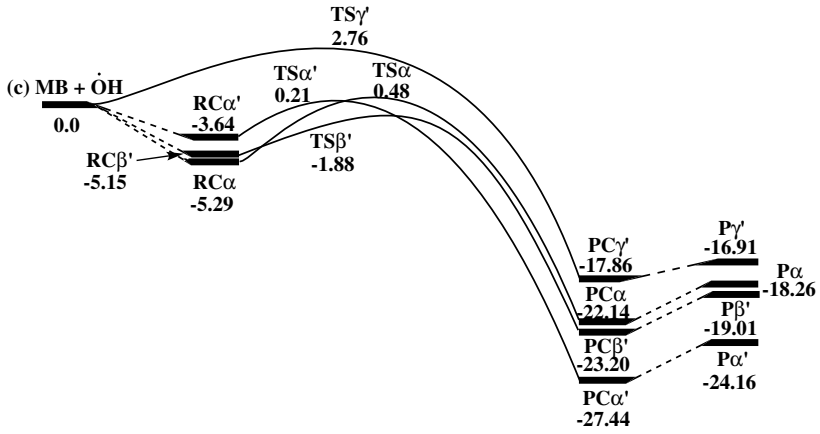

Figure 6: Potential Energy Surface of the reactions of MB + ȮH radicals calculated with the G3 method, in kcal mol^{-1}.

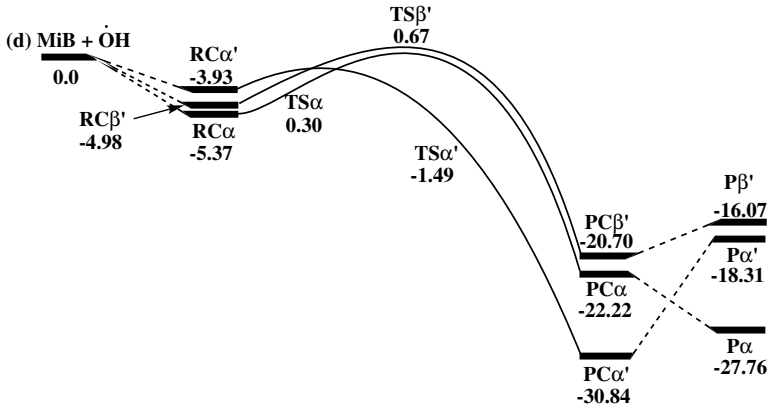

Figure 7: Potential Energy Surface of the reactions of MiB + ȮH radicals calculated with the G3 method, in kcal mol^{-1}.

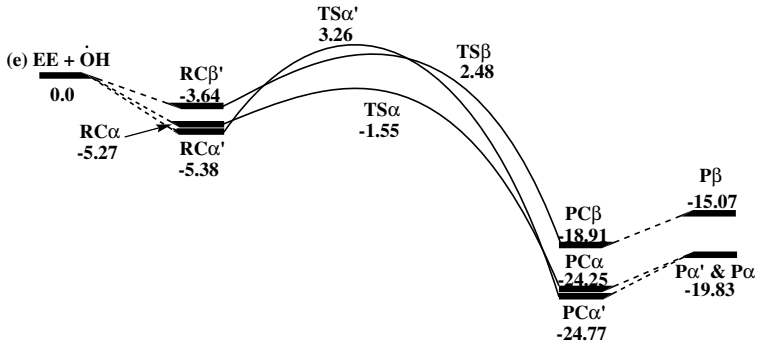

Figure 8: Potential Energy Surface of the reactions of EE + ȮH radicals calculated with the G3 method, in kcal mol^{-1}.

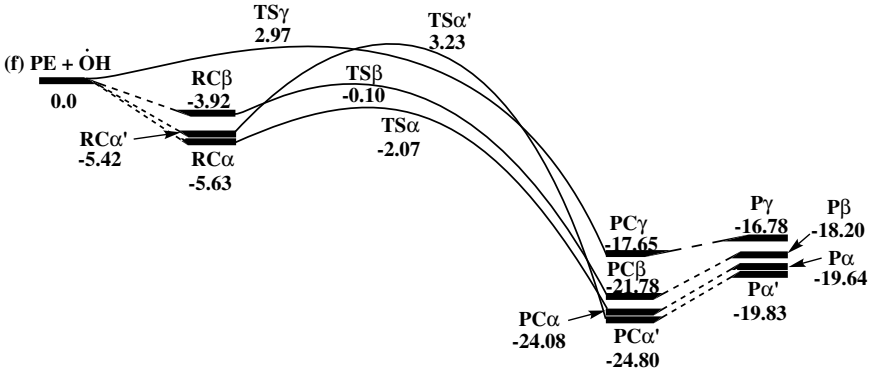

Figure 9: Potential Energy Surface of the reactions of PE + ȮH radicals calculated with the G3 method, in kcal mol^{-1}.

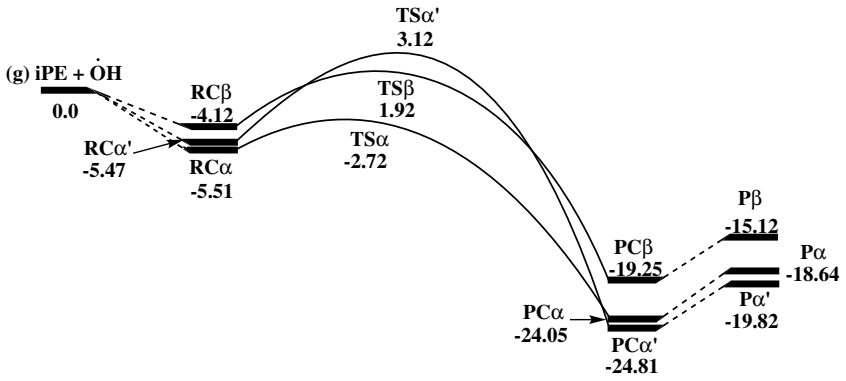

Figure 10: Potential Energy Surface of the reactions of iPE + ȮH radicals calculated with the G3 method, in kcal mol^{-1}.

when an ȮH radical approaches the molecule where it will form a RC in the entrance channel and a PC in the exit channel. Abstraction of a primary (1°) hydrogen atom at the α' position of ME, EE, PE and iPE forms a reactant complex (RCα') at energies of -5.47 to -5.24 kcal mol^{-1} in the entrance channel and a product complex (PCα') at energies of -24.81 to -24.62 kcal mol^{-1} in the exit channel. It proceeds through the corresponding transition states (TSα') with an electronic energy relative to the reactants of 3.43, 3.26, 3.23 and 3.12 kcal mol^{-1} for ME, EE, PE and iPE, respectively. At the same position, abstraction of a secondary (2°) hydrogen atom in MP and MB and a tertiary (3°) hydrogen atom in MiB occurs similar to a 1° hydrogen atom and the transition states formed have relative electronic energies of 0.65, 0.21 and -1.49 kcal mol^{-1}, respectively. At the α position, abstraction of a hydrogen atom occurs similar to the α' position with relative electronic energies for the transition states (TSα) ranging from 0.30 to 0.69 kcal mol^{-1} (1° hydrogen atom), -2.07 to -1.55 kcal mol^{-1} (2° hydrogen atom) and -2.72 kcal mol^{-1} (3° hydrogen atom). A similar trend was observed at the γ', β', β and γ positions for abstraction of a 1° or 2° hydrogen atom, Table 1.

Table 2 shows the bond dissociation energies (BDEs) for several esters in this work and a comparison with the BDEs calculated by Oyeyemi *et al.*[22] and El-Nahas *et al.*,[23] in kcal mol^{-1}. A trend is observed where the BDE of a 1° hydrogen atom is similar in both α' and α positions in this work. However, the same is not observed for a 2° hydrogen atom where the BDE is lower at

the α' than at the α position, by about 4 kcal mol^{-1}. We also observe that at the α position, both 1° and 2° hydrogen atoms have similar BDEs which was also observed in the studies by Oyeyemi *et al.* and El-Nahas *et al.* When comparing these BDEs to our calculated electronic energy barriers for abstraction (Table 1) we observe the opposite trend where the energy barriers for abstraction of a 1° and 2° hydrogen atoms at the α' position are higher than at the α position, by about 2–3 kcal mol^{-1}.

Table 2: Bond dissociation energies (BDEs) for several esters in this work and the ones calculated by Oyeyemi *et al.*[22] and El-Nahas *et al.*,[23] in kcal mol^{-1}.

	Method	α' 1° H-atom	α' 2° H-atom	α 1° H-atom	α 2° H-atom
This work	CCSD(T)/cc-pVTZ	ME, 97.3	MP, 92.3	ME, 97.6	EE, 96.1
	G3	ME, 97.0	MP, 92.3	ME, 98.6	EE, 97.0
Oyeyemi *et al.*[22]	MRACPF2		EP, 93.2	MP, 100.9	EP, 99.6
El-Nahas *et al.*[23]	CBS-QB3		EP, 94.2	MB, 98.9	EP 97.3

Rate Constant Calculations

We have calculated the high-pressure limit rate constants in the temperature range from 500 to 2200 K. Figures 11–13 show our current results and we have compared them to the rate constants calculated in our previous work for abstraction from ketones[10] and those for alkanes calculated by Sivaramakrishnan *et al.*[24] The low-frequency torsional modes were determined with the use of the Pitzer–Gwinn-like[25] approximation. In our previous works on esters,[1] ketones,[8–10] ethers[11,12] and alcohols,[13,14] we have used the one dimensional hindered rotor treatment (1D-HR) in our rate constant calculations. For abstraction of a hydrogen atom at the alpha position of *n*-butanol when reacting with an $H\dot{O}_2$ radical,[14] a comparison was performed between our rate constant results obtained with the use of the 1D-HR and the ones obtained by Truhlar and co-workers[26,27] using the multi-structure method. $H\dot{O}_2$ radicals are in high concentration between 800 K and 1300 K and high pressures (>10 atm).[8] In this temperature range, it was observed that the results were quite similar where the rate constants calculated by Zhou *et al.*[14] are within 20% to 40% of those calculated by Truhlar and co-workers.[26]

Herein, we use the same nomenclature (R′ and R) as in our previous work on esters + $H\dot{O}_2$ radicals[1] in order to differentiate between the two sides of the ester molecule (Figure 1). Figures 11(a)–12(b) detail the results of our calculations at the different positions (α', β' and γ') of the R′ side of the molecule and Figures 12(c)–13(d) at the R side (α, β and γ). Our calculations are compared with the results from our previous work on ketones[10] and with alkanes calculated by Sivaramakrishnan *et al.*[24]

At the R′ side of the esters, abstraction of a 1° (Figure 11(a)), 2° (Figure 11(b)) or 3° (Figure 11(c)) hydrogen atom by an $\dot{O}H$ radical at the α' position is slower than the ketones[10] by about a factor 2 at 600 K for all types of hydrogen atom. At 2200 K, abstraction of a 1° hydrogen atom is similar to ketones and slower by about 40% for 2° and 3° hydrogen atoms. At the β' position, abstraction of a 1° hydrogen atom (Figure 11(d)) is slower than for ketones by about a factor of 2 from 500 to 2200 K.

At the R side of the molecule, abstraction of a hydrogen atom at the α position is similar to the corresponding position in a ketone.[10] Abstraction of a 1° (Figure 12(c)) and 3° (Figure 13(a)) hydrogen atom is slower than for ketones[10] by about 40 to 70% from 600–2200 K, while abstraction of a 2° hydrogen atom (Figure 12(d)) differs by about 30% within the same temperature range. When comparing the reactivity of a 1° (Figure 13(b)) hydrogen atom at the β position, abstraction is slower than for ketones[10] by a factor of 11 at 500 K, becoming closer in reactivity as the temperature increases, remaining slower by 60% at 2200 K.

When compared to alkanes,[24] abstraction of a 1° hydrogen atom at the α' position (Figure 11(a)) of the esters is slower by a factor of 3 at 500 K and is 80% slower at 2200 K. Abstraction of a 2° hydrogen atom (Figure 11(b)) is slower by about a factor of 2 at 700 K and becomes similar to an alkane as the temperature increases. Abstraction of a 3° hydrogen atom (Figure 11(c)) is faster than for alkanes[24] by about 70% at 500 K, and becomes similar in reactivity as it nears a temperature of 2200 K. At the β' position, abstraction of a 1° hydrogen atom (Figure 11(d)) is slower than for alkanes[24] by about a factor of 3 from 600 to 2200 K while abstraction of a 2° hydrogen atom (Figure 12(a)) is slower by about a factor of 2 from 700 to 2200 K. At the γ' position, our

results (Figure 12(b)) are similar to abstraction from alkanes.[24] The same is observed at the γ position (Figure 13(d)) at the R side of the ester. At the α position, abstraction of a 1° hydrogen atom (Figure 12(c)) is slower than for alkanes[24] by about a factor of 3 from 700 to 1600 K, decreasing to a factor of 2 slower at 2200 K. Abstraction of a 2° hydrogen atom (Figure 12(d)) is faster than alkanes[24] by 30% at 500 K. Above 500 K, alkanes[24] are about 10 to 60% faster. Abstraction of a 3° hydrogen atom (Figure 13(a)) is faster at 500 K by about a factor of 3, becoming more similar as the temperature increases. At the β position, the reactivity of a 1° hydrogen atom (Figure 13(b)) is slower than in alkanes[24] by a factor of 8 and 2 at 500 and 2200 K, respectively. Abstraction of a 2° hydrogen atom (Figure 13(c)) is slower by a factor of 4 at 500 K, decreasing to 50% at 2200 K.

In our previous works, when we compared our results on the esters + $H\dot{O}_2$ radicals[1] with ketones + $H\dot{O}_2$ radicals,[8,9] we observed that the calculated rate constants were very similar. However, when comparing our results in this work we observe that abstraction of a hydrogen atom of the esters by an $\dot{O}H$ radical is generally slower than when abstracting from the corresponding position in ketones.[10] As the $H\dot{O}_2$ radical is a heavier radical than the $\dot{O}H$ radical, the interactions between the $\dot{O}H$ radical and the functional group (RC=OR′ in ketones or RC=OOR′ in esters) is more significant than the interactions of the $H\dot{O}_2$ radical with the same functional group. Both $\dot{O}H$ and $H\dot{O}_2$ radicals, when abstracting a hydrogen atom from the ester molecule through the transition state structure(s), form(s) a hydrogen bond between an oxygen atom of the functional group and the hydrogen atom on the radical and this is considered when determining the hindrance potentials for the transition states. In the case of abstraction by $\dot{O}H$ radicals these interactions have a bigger impact on our rate constant calculations compared to those for abstraction by $H\dot{O}_2$ radicals which is due to the $\dot{O}H$ radicals being more sensitive to these hydrogen bond interactions, as well as the calculated relative electronic energies, than the $H\dot{O}_2$ radicals. These are the reasons for the slower reactivity in our results in this work when comparing to our previous work.[10]

Figure 14 shows a comparison of the reactivity of 1°, 2° and 3° hydrogen atoms when undergoing abstraction by an $\dot{O}H$ radical, at both sides of the ester molecule. As expected, abstraction of a tertiary hydrogen atom is the fastest and that of a primary one is the slowest (Figures 14(a)

and 14(b)). At high temperatures, the reactivity is similar at both sides of the ester molecule. At low temperatures, the difference in reactivity is due to the higher energies of the transition states at the α' and β positions compared to the α and β' positions (Table 1). For the α' position, abstraction of a 1°, 2° or 3° hydrogen atom is slower than at the α site by approximately a factor of 2 at 500 K (Figure 14(a)). Abstraction of a 1° or 2° hydrogen atom at the β' position is faster than at the β site by a factor of 5 at the same temperature. At the γ' and γ positions (Figure 14(c)), we do not observe this difference in the calculated energies of the transition states and, therefore, the reactivity is similar from 500 to 2200 K.

Tables 3–5 show the fit parameters of our rate constant results on a per hydrogen atom basis (Table 3), average (Table 4) and total (Table 5).

Table 3: Rate constants Arrhenius fit parameters (A, n and E), in cm^3 mol^{-1} s^{-1}, at each position of the esters in this work, on a per hydrogen atom basis.

Position	H-Atom Type	Species	A	n	E
	1°	ME	9.07×10^{-1}	3.73	−1229.
	1°	EE	$1.51 \times 10^{+0}$	3.68	−1257.
	1°	PE	$4.29 \times 10^{+0}$	3.54	−1080.
α'	1°	iPE	$2.61 \times 10^{+0}$	3.59	−1291.
	2°	MP	$1.21 \times 10^{+2}$	3.14	−2192.
	2°	MB	$4.87 \times 10^{+2}$	2.94	−2107.
	3°	MiB	$4.23 \times 10^{+3}$	2.70	−3199.
	1°	MP	9.21×10^{-3}	4.22	−3455.
β'	2°	MB	3.88×10^{-1}	3.76	−4890.
	1°	MiB	1.09×10^{-1}	3.91	−2805.
γ'	1°	MB	$1.46 \times 10^{+4}$	2.61	750.
	1°	ME	5.56×10^{-3}	4.31	−3401.
	1°	MP	1.03×10^{-2}	4.24	−3397.
	1°	MB	6.11×10^{-3}	4.28	−3443.
α	1°	MiB	9.17×10^{-3}	4.26	−3591.
	2°	EE	$1.34 \times 10^{+0}$	3.66	−4095.
	2°	PE	$1.46 \times 10^{+0}$	3.67	−4159.
	3°	iPE	$4.70 \times 10^{+0}$	3.52	−5487.
	1°	EE	$2.27 \times 10^{+0}$	3.62	−273.
β	2°	PE	$4.25 \times 10^{+1}$	3.26	−1695.
	1°	iPE	2.61×10^{-1}	3.87	−505.
γ	1°	PE	$2.83 \times 10^{+4}$	2.57	941.

$k = A \times T^n \times \exp(-E/RT)$, where $R = 1.987$ cal K^{-1} mol^{-1}

Figure 15 details a comparison of the total rate constants for ME, MP and MB in this work

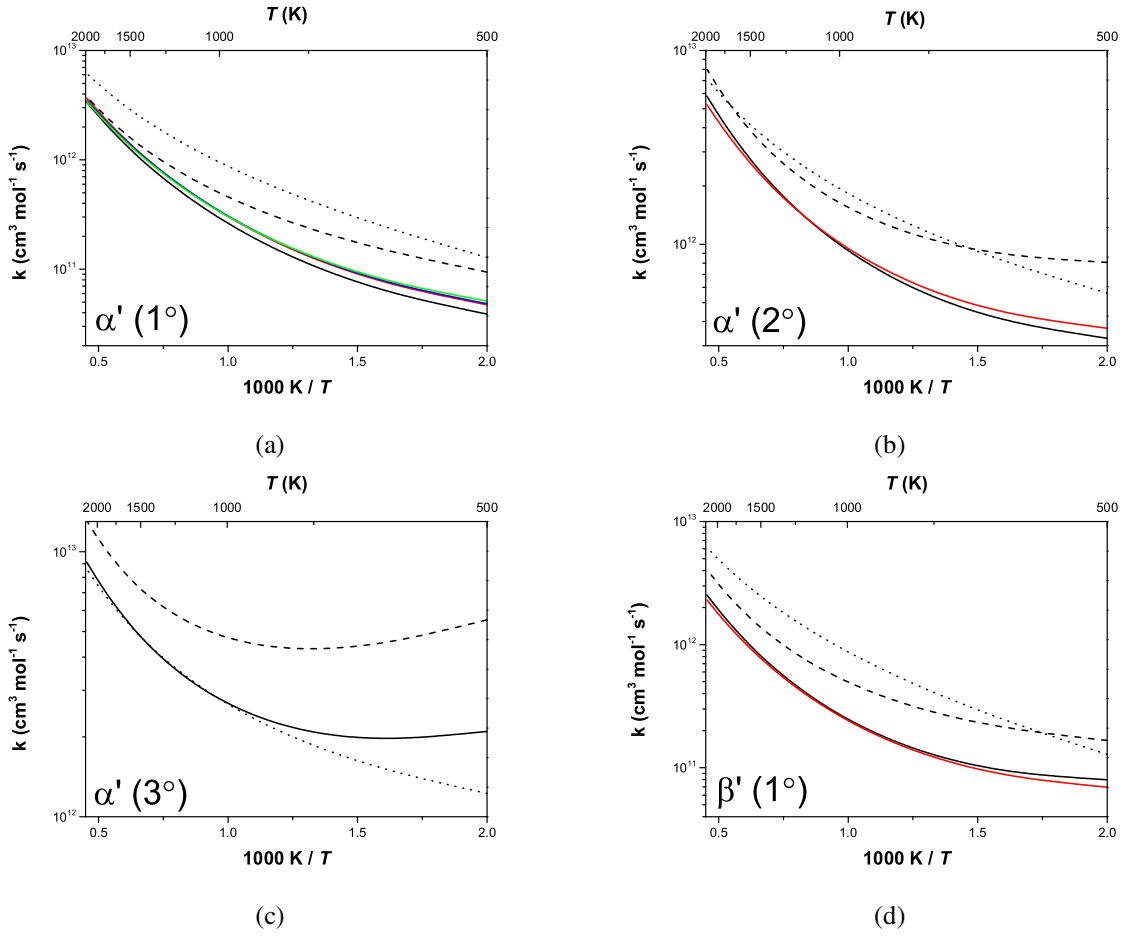

Figure 11: Rate constants comparison at the α' (1°, 2° and 3° hydrogen atoms) and β' (1° hydrogen atom) positions relative to the RC=OOR′ group, in $cm^3\ mol^{-1}\ s^{-1}$. (a) ME (black), EE (red), PE (blue), iPE (green) (b) MP (black), MB (red) (c) MiB (black) (d) MP (black), MiB (red); ketones + $\dot{O}H$[10] (dashed) and alkanes + $\dot{O}H$[24] (dotted).

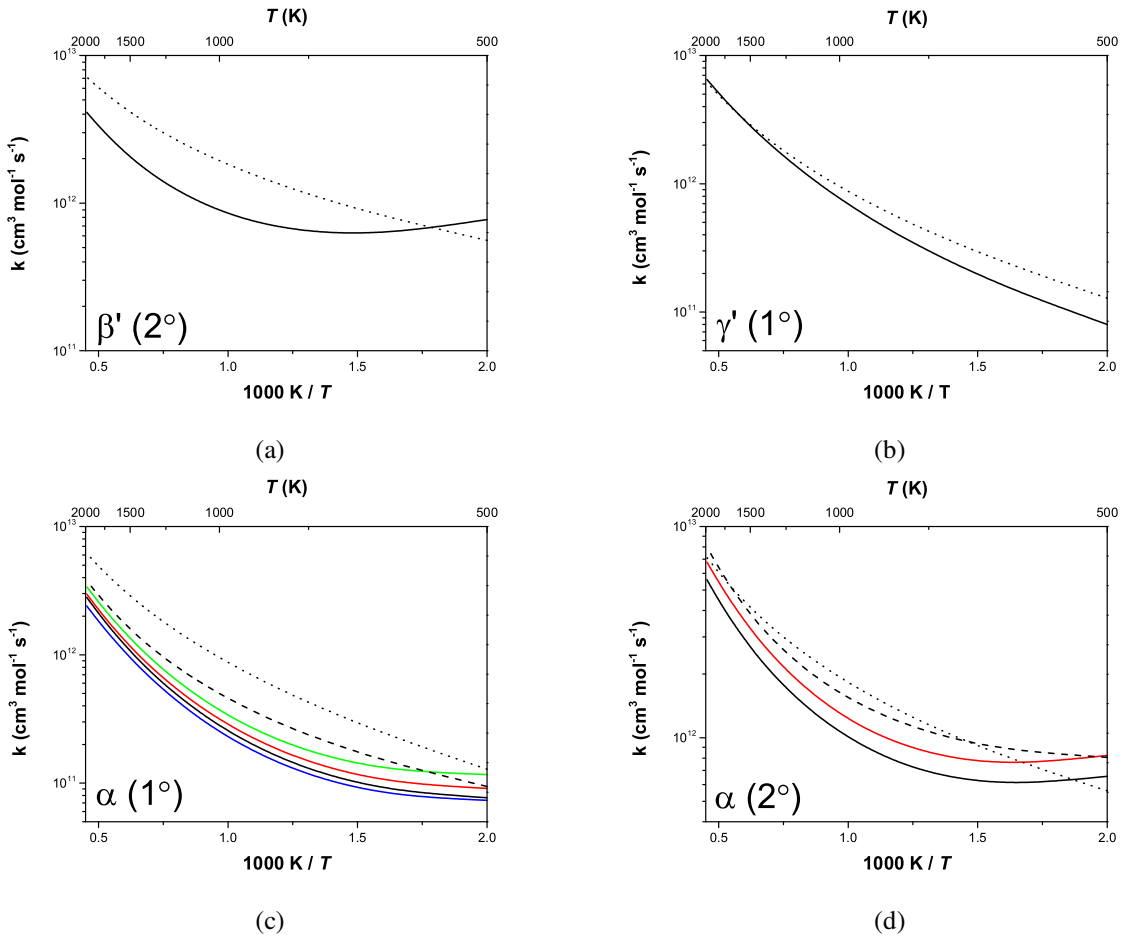

Figure 12: Rate constants comparison at the β' (2° hydrogen atom), γ' (1° hydrogen atom) and α (1° and 2° hydrogen atoms) positions relative to the RC=OOR′ group, in cm^3 mol^{-1} s^{-1}. (a) MB (black) (b) MB (black) (c) ME (black), MP (red), MB (blue), MiB (green) (d) EE (black), PE (red); ketones + $\dot{O}H$[10] (dashed) and alkanes + $\dot{O}H$[24] (dotted).

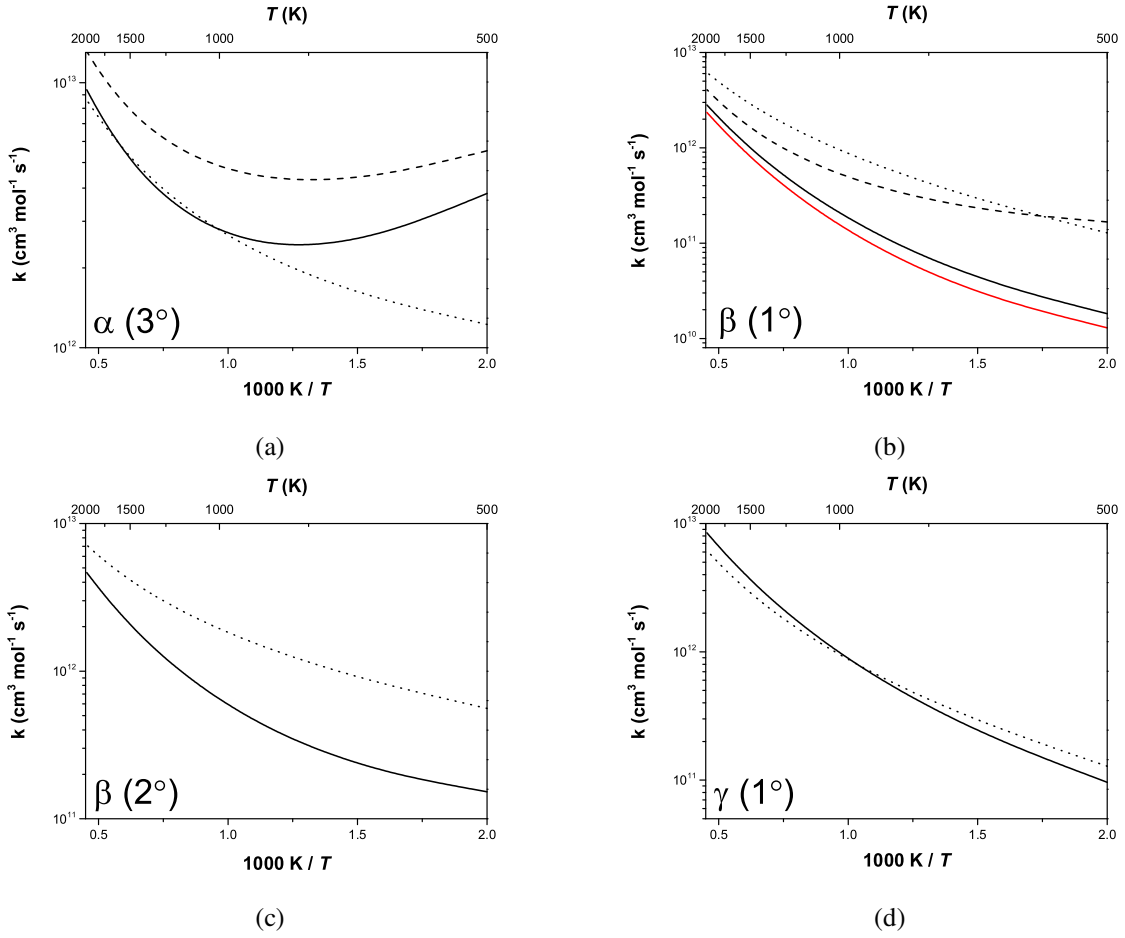

Figure 13: Rate constants comparison at the α (3° hydrogen atom), β (1° and 2° hydrogen atoms) and γ (1° hydrogen atom) positions relative to the RC=OOR′ group, in cm^3 mol^{-1} s^{-1}. (a) iPE (black) (b) EE (black), iPE (red) (c) PE (black) (d) PE (black); ketones + $\dot{O}H$[10] (dashed) and alkanes + $\dot{O}H$[24] (dotted).

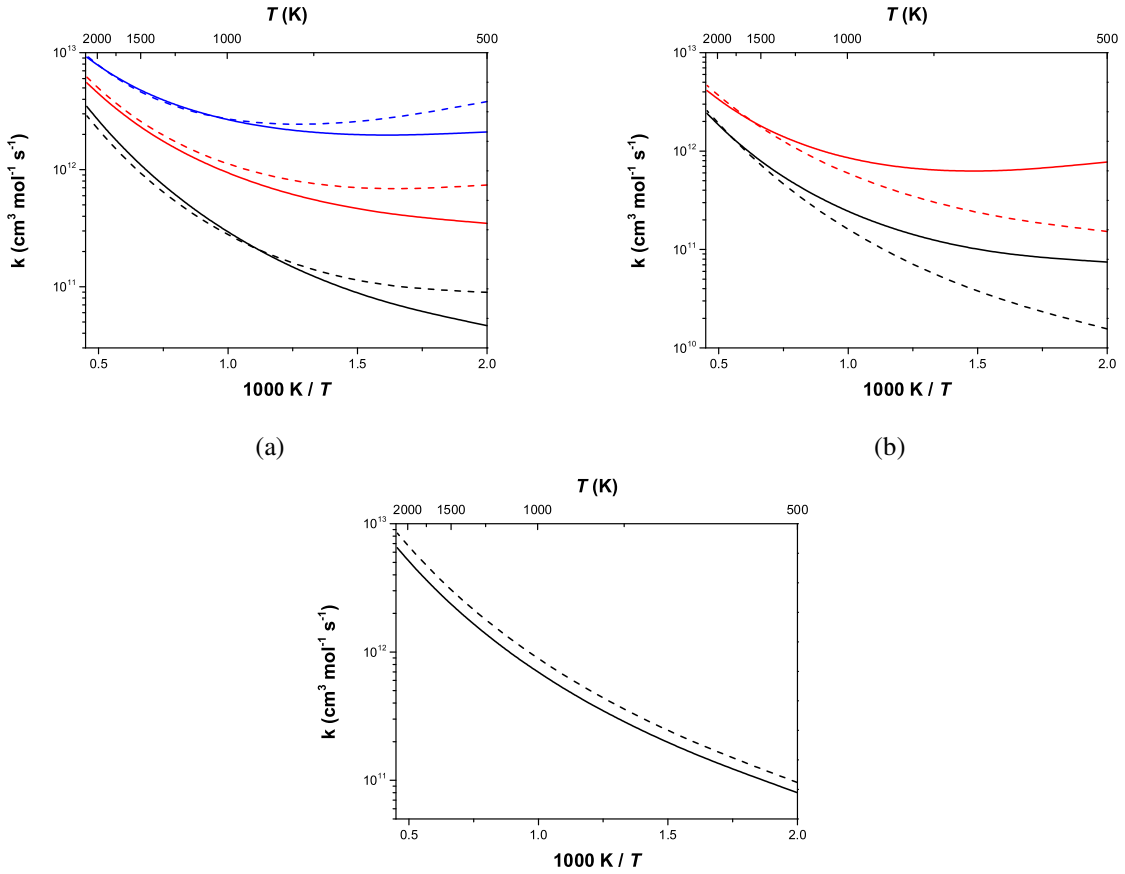

Figure 14: Reactivity of 1° (black), 2° (red) and 3° (blue) hydrogen atoms at the R′ (solid lines) and R (dashed lines) sides of the esters: (a) α' and α positions; (b) β' and β positions and (c) γ' and γ positions.

Table 4: Average Arrhenius fit parameters (A, n and E), on a per-hydrogen atom basis according to hydrogen atom type (1°, 2° or 3°) and position (α', β', γ', α, β or γ) relative to the functional group of the ester. Values in units of cm^3 mol^{-1} s^{-1}.

Position	H-Atom Type	A	n	E
α'	1°	$1.96 \times 10^{+0}$	3.64	−1222.
	2°	$2.33 \times 10^{+2}$	3.04	−2160.
	3°	$4.23 \times 10^{+3}$	2.70	−3199.
β'	1°	3.04×10^{-2}	4.07	−3142.
	2°	3.88×10^{-1}	3.76	−4890.
γ'	1°	$1.46 \times 10^{+4}$	2.61	750.
α	1°	7.47×10^{-3}	4.27	−3473.
	2°	$1.40 \times 10^{+0}$	3.67	−4131.
	3°	$4.70 \times 10^{+0}$	3.52	−5487.
β	1°	8.63×10^{-1}	3.73	−379.
	2°	$4.25 \times 10^{+1}$	3.26	−1695.
γ	1°	$2.83 \times 10^{+4}$	2.57	941.

$k = A \times T^n \times \exp(-E/RT)$, where R = 1.987 cal K^{-1} mol^{-1}

Table 5: A, n and E parameters for the total rate constants in this work. Values in units of cm^3 mol^{-1} s^{-1}.

Species	A	n	E
ME	2.02×10^{-1}	4.11	−2538.
MP	$5.78 \times 10^{+0}$	3.72	−2876.
MB	$7.80 \times 10^{+0}$	3.73	−3310.
MiB	$2.58 \times 10^{+0}$	3.81	−4020.
EE	7.29×10^{-2}	4.26	−4072.
PE	$1.49 \times 10^{+1}$	3.70	−2723.
iPE	3.98×10^{-4}	4.88	−6417.

$k = A \times T^n \times \exp(-E/RT)$, where R = 1.987 cal K^{-1} mol^{-1}

with that from the experimental data obtained by Lam *et al.*[2] Compared to the experimental values obtained by Lam *et al.*,[2] our theoretical results are slower by about a factor of 2 for ME (Figure 15(a)), from 876 to 1371 K, and slower by about 40 to 50% for MP (Figure 15(b)), from 909 to 1341 K, and MB (Figure 15(c)), from 925 to 1355 K. A comparison to the estimated rate constants by Westbrook *et al.*,[3] Dooley *et al.*,[4] Fisher *et al.*,[5] Hakka *et al.*[6] and Diévart *et al.*[7] has also been performed and it is shown that the rate constants calculated in this work describe more accurately the temperature dependence of the title reactions.

Also depicted in Figure 15 are rate constants where we have decreased (dashed red line) and increased (dotted red line) the electronic energy barrier height of the transition states by 1.0 kcal

mol^{-1}, which is within the uncertainty of the calculations. Decreasing the activation energy by this amount leads to better agreement with the experimental data obtained by Lam *et al.*,[2] Figure 15. We observe that these adjusted rate constants are almost identical to the experimental values within their range of measurement, with the largest differences being 29% at 1126 K for ME, 16% at 909 K for MP and 27% at 897 K for MB.

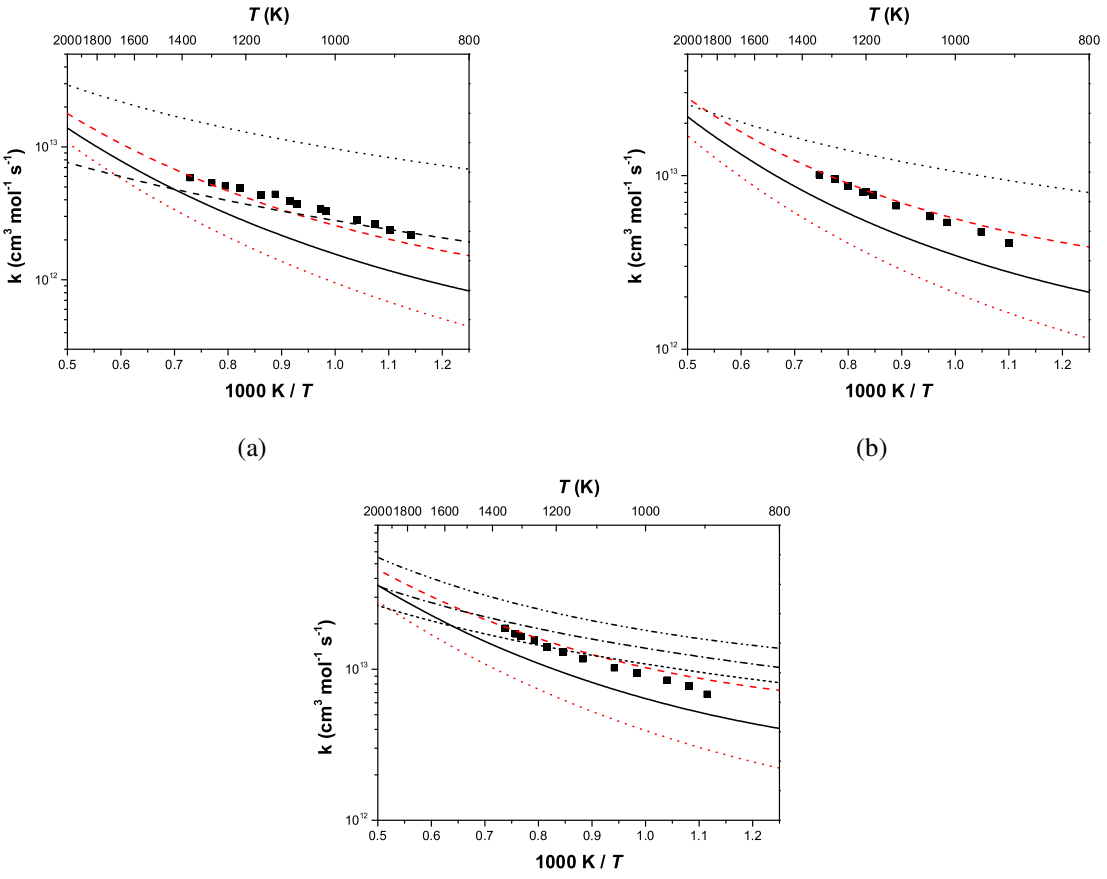

Figure 15: Comparison of the total rate constants calculated in this work, (–), (- -) and (...) with the experimental values obtained by Lam *et al.*[2] (■) and the estimated values by Dooley *et al.*[4] (dash-dotted black line), Westbrook *et al.*[3] (dashed black line), Fisher *et al.*[5] (short dashed black line), Hakka *et al.*[6] (dash-dot-dotted black line) and Diévart *et al.*[7] (dotted black line). (–) are our reported total rate constants in this work for (a) ME, (b) MP and (c) MB. (- -) and (...) are the total rate constants using the same treatment as the reported rate constants (–) where only the electronic energy barrier height of the transition states was changed by ± 1 kcal mol^{-1}.

In our previous works on esters[1] and ethers[12] + $\dot{H}O_2$ radicals, we estimated an overall uncer-

tainty of a factor of 2.5 in our rate constant calculations. This was based on the results calculated using VariFlex, CanTherm and MultiWell in our previous work on *n*-butanol + $\dot{C}H_3$ radicals[28] and based on the suggestion by Goldsmith *et al.* that simple abstraction reactions have an uncertainty of a factor of 2 to 3.[29] Also, the conclusions in this work support this overall estimated uncertainty where our calculated rate constant results are within a factor of 2 for ME and 40 to 50% for MP and MB, from the experimental results obtained by Lam *et al.*[2]

Branching Ratios

Figure 16 shows the calculated branching ratios for each position on each ester in the title reactions. Figure 16(a) details the branching ratio for ME and the α channel dominates from 500 to 900 K. Above 900 K the α' channel becomes dominant. In Figure 16(b) we detail the branching ratio for MP and the α' channel dominates from 500 to 2200 K. Channels α and β become more important as the temperature increases. For MB (Figure 16(c)), β' channel dominates from 500 to 800 K. The γ' channel then takes over and dominates from 1000 to 2200 K. Figure 16(d) details the reactivity of MiB and we observe that the α' channel is dominant from 500 to 1500 K, above which the β' channel is dominant, followed by the α channel. In Figure 16(e) we give the branching ratio for EE and channel α is dominant from 500 to 2200 K. Reactivity of the other two channels (α' and β) increases with temperature and at 2200 K the reactivity of the β channel is similar to the α channel. Figure 16(f) shows the reactivity of PE and the γ channel dominates from 1000 to 2200 K. At 2200 K the reactivity of the α channel is nearer to the reactivity of the β and α' channels, however, below 1000 K the α channel is dominant. For iPE (Figure 16(g)), abstraction from the α channel dominates from 500 to 1600 K. The reactivity of the other two channels becomes more important as the temperature increases and above 1600 K abstraction from the β channel is dominant.

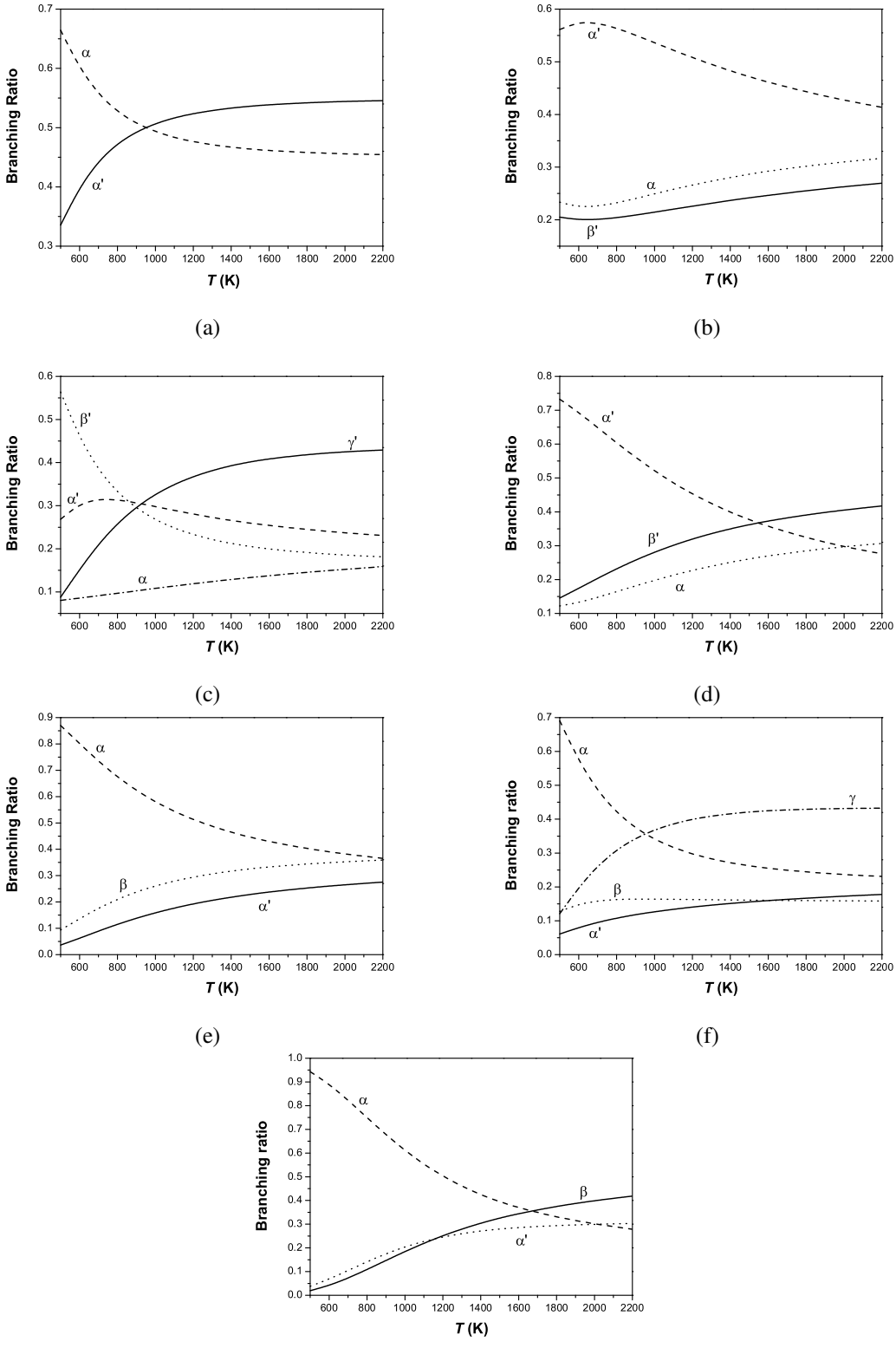

Figure 16: Estimated branching ratios, in the temperature range from 500–2200 K, for each site of each ester in this work: (a) ME; (b) MP; (c) MB; (d) MiB; (e) EE; (f) PE; (g) iPE.

Conclusions

We have calculated rate constants for hydrogen atom abstraction reactions by ȮH radicals on esters, including ME, MP, MB, MiB, EE, PE and iPE. As in our previous works on abstraction by ȮH and HȮ$_2$ radicals from ketones,[8–10] esters,[1] ethers,[11,12] and alcohols,[13,14] complexes were found in both the entrance and exit channels. Conventional transition state theory was used to calculate the rate constants at the high-pressure limit and our results were compared to ketones[10] and alkanes[24] + ȮH radical reactions. When an ȮH radical abstracts a hydrogen atom from the α', β', α and β positions, the rate constants are generally slower than at the corresponding sites in the ketones[10] and alkanes.[24] At the γ' and γ positions the reactivity is most similar to an alkane.

The ȮH radical is lighter than an HȮ$_2$ radical which has an effect when they interact with the functional group (RC=OR′ in ketones or RC=OOR′ in esters) of the oxygenated molecule. Due to the larger distance of the ȮH radical from the functional group when undergoing abstraction at the γ' and γ positions, the formation of a hydrogen bond between the hydrogen atom of the hydroxyl radical and one of the oxygen atoms of the RC=OOR′ group does not occur. The same is not true at the α', β', α and β positions and a hydrogen bond is formed in the transition states when ȮH radicals interact with the oxygenated molecule. This hydrogen bond interaction has a more significant impact when the esters react with the ȮH radical than with the HȮ$_2$ radical. When determining the hindrance potentials in this work, the oxygen from the alkoxy moiety of the ester interacts with the hydrogen atom of the ȮH radical. Due to the higher sensitivity of an ȮH radical compared to an HȮ$_2$ radical, the lower relative electronic energies and these hydrogen bond interactions in some of the reaction channels in this work have a bigger impact on our calculated rate constant results.

Based on our results, we observe that at high temperatures reactivity is similar on both sides of an ester. At low temperatures, the lower relative electronic energies of some transition states increase the reactivity for abstraction at the α' and β positions compared to the α and β' positions (Figure 14).

We have performed a comparison of the total rate constants calculated here with the experi-

mental results measured by Lam *et al.*[2] and they are within a factor of 2 of one another for ME and within 40 to 50% for MP and MB which is within our estimated uncertainty of a factor of 2.5. Our calculations are also compared to the estimated rate constants by Dooley *et al.*,[4] Fisher *et al.*,[5] Hakka *et al.*[6] and Diévart *et al.*[7] and we conclude that the rate constants calculated in this work more accurately reflect the temperature dependence measured by Lam *et al.*

A branching ratio analysis has also been carried out and abstraction at the γ' and γ positions dominate above about 1000 K. At low temperatures, the type of hydrogen atom (1°, 2° and 3°) has a bigger influence on reactivity and a 3° hydrogen atom dominates over a 2° one which dominates over a 1° one.

Acknowledgement

This work was supported by Science Foundation Ireland under grant number [08/IN1./I2055]. Computational resources were provided by the Irish Center for High-End Computing (ICHEC).

Supporting Information Available

Table S1 provides details of the CCSD(T)/cc-pVDZ (TZ, QZ) and CCSD(T)/CBS relative electronic energy calculations for the hydrogen atom abstraction reactions of ME with an $\dot{O}H$ radical and Table S2 provides the geometry co-ordinates and frequencies for the reactants and transitions states in the title reactions.

This material is available free of charge via the Internet at `http://pubs.acs.org/`.

References

(1) Mendes, J.; Zhou, C.-W.; Curran, H. J. Theoretical And Kinetic Study Of The Hydrogen Atom Abstraction Reactions Of Esters With $H\dot{O}_2$ Radicals. *J. Phys. Chem. A* **2013**, *117*, 14006–14018.

(2) Lam, K.-Y.; Davidson, D. F.; Hanson, R. K. High-Temperature Measurements Of The

Reactions Of ȮH With Small Methyl Esters: Methyl Formate, Methyl Acetate, Methyl Propanoate, And Methyl Butanoate. *J. Phys. Chem. A* **2012**, *116*, 12229–12241.

(3) Westbrook, C.; Pitz, W.; Westmoreland, P.; Dryer, F.; Chaos, M.; Osswald, P.; Kohse-Höinghaus, K.; Cool, T.; Wang, J.; Yang, B.; *et al.*, A Detailed Chemical Kinetic Reaction Mechanism For Oxidation Of Four Small Alkyl Esters In Laminar Premixed Flames. *Proc. Comb. Inst.* **2009**, *32*, 221–228.

(4) Dooley, S.; Curran, H.; Simmie, J. Autoignition Measurements And A Validated Kinetic Model For The Biodiesel Surrogate, Methyl Butanoate. *Combustion and Flame* **2008**, *153*, 2–32.

(5) Fisher, E.; Pitz, W.; Curran, H.; Westbrook, C. Detailed Chemical Kinetic Mechanisms For Combustion Of Oxygenated Fuels. *Proc. Comb. Inst.* **2000**, *28*, 1579–1586.

(6) Hakka, M. H.; Bennadji, H.; Biet, J.; Yahyaoui, M.; Sirjean, B.; Warth, V.; Coniglio, L.; Herbinet, O.; Glaude, P. A.; Billaud, F.; *et al.*, Oxidation Of Methyl And Ethyl Butanoates. *Int. J. Chem. Kinet.* **2010**, *42*, 226–252.

(7) Diévart, P.; Won, S. H.; Gong, J.; Dooley, S.; Ju, Y. A Comparative Study Of The Chemical Kinetic Characteristics Of Small Methyl Esters In Diffusion Flame Extinction. *Proc. Comb. Inst.* **2013**, *34*, 821–829.

(8) Mendes, J.; Zhou, C.-W.; Curran, H. J. Theoretical And Kinetic Study Of The Reactions Of Ketones With $H\dot{O}_2$ Radicals. Part I: Abstraction Reaction Channels. *J. Phys. Chem. A* **2013**, *117*, 4515–4525.

(9) Mendes, J.; Zhou, C.-W.; Curran, H. J. Correction to Theoretical And Kinetic Study Of The Reactions Of Ketones With $H\dot{O}_2$ Radicals. Part I: Abstraction Reaction Channels. *J. Phys. Chem. A* **2014**, *118*, 331–331.

(10) Zhou, C.-W.; Simmie, J. M.; Curran, H. J. Ab Initio And Kinetic Study Of The Reaction Of Ketones With $\dot{O}H$ for T=500–2000 K. Part I: Hydrogen-Abstraction From $H_3CC(O)CH_{3-x}(CH_3)_x$, x = 0 → 2. *Phys. Chem. Chem. Phys.* **2011**, *13*, 11175–11192.

(11) Zhou, C.-W.; Simmie, J. M.; Curran, H. J. An Ab Initio/Rice-Ramsperger-Kassel-Marcus Study Of The Hydrogen-Abstraction Reactions Of Methyl Ethers, $H_3COCH_{3-x}(CH_3)_x$, x = 0–2, By $\dot{O}H$; Mechanism And Kinetics. *Phys. Chem. Chem. Phys.* **2010**, *12*, 7221–7233.

(12) Mendes, J.; Zhou, C.-W.; Curran, H. J. Rate Constant Calculations Of H-Atom Abstraction Reactions From Ethers By $H\dot{O}_2$ Radicals. *J. Phys. Chem. A* **2014**, *118*, 1300–1308.

(13) Zhou, C.-W.; Simmie, J. M.; Curran, H. J. Rate Constants For Hydrogen-Abstraction By $\dot{O}H$ From *n*-Butanol. *Combustion and Flame* **2011**, *158*, 726–731, Special Issue on Kinetics.

(14) Zhou, C.-W.; Simmie, J. M.; Curran, H. J. Rate Constants For Hydrogen Abstraction By $H\dot{O}_2$ From *n*-Butanol. *Int. J. Chem. Kinet.* **2012**, *44*, 155–164.

(15) Frisch, M. J.; Trucks, G. W.; Schlegel, H. B.; Scuseria, G. E.; Robb, M. A.; Cheeseman, J. R.; Scalmani, G.; Barone, V.; Mennucci, B.; Petersson, G. A.; *et al.*, Gaussian 09 Revision A.1. Gaussian Inc. Wallingford CT 2009.

(16) Peterson, K. A.; Woon, D. E.; Dunning, T. H. Benchmark Calculations With Correlated Molecular Wave-Functions .4. The Classical Barrier Height Of The $H+H_2 \rightarrow H_2+H$ Reaction. *J. Chem. Phys.* **1994**, *100*, 7410–7415.

(17) ChemCraft v1.6 http://www.chemcraftprog.com/.

(18) Glasstone, S.; Laidler, K. J.; Eyring, H. Theory of Rate Processes. *McGraw-Hill: New York* **1941**,

(19) Eckart, C. The Penetration Of A Potential Barrier By Electrons. *Phys. Rev.* **1930**, *35*, 1303–1309.

(20) Klippenstein, S. J.; Wagner, A. F.; Dunbar, R. C.; Wardlaw, D. M.; Robertson, S. H. VariFlex, version 2.02m. Argonne National Laboratory, Argonne, IL, 1999.

(21) Georgievskii, Y.; Klippenstein, S. J. Strange Kinetics of the C_2H_6 + CN Reaction Explained. *J. Phys. Chem. A* **2007**, *111*, 3802–3811.

(22) Oyeyemi, V. B.; Keith, J. A.; Carter, E. A. Accurate Bond Energies of Biodiesel Methyl Esters from Multireference Averaged Coupled-Pair Functional Calculations. *J. Phys. Chem. A* **0**, *0*, null.

(23) El-Nahas, A. M.; Navarro, M. V.; Simmie, J. M.; Bozzelli, J. W.; Curran, H. J.; Dooley, S.; Metcalfe, W. Enthalpies of Formation, Bond Dissociation Energies and Reaction Paths for the Decomposition of Model Biofuels: Ethyl Propanoate and Methyl Butanoate. *J. Phys. Chem. A* **2007**, *111*, 3727–3739.

(24) Sivaramakrishnan, R.; Michael, J. V. Rate Constants for ȮH With Selected Large Alkanes: Shock-Tube Measurements And An Improved Group Scheme. *J. Phys. Chem. A* **2009**, *113*, 5047–5060.

(25) Pitzer, K. S.; Gwinn, W. D. Energy Levels And Thermodynamic Functions For Molecules With Internal Rotation I. Rigid Frame With Attached Tops. *J. Chem. Phys.* **1942**, *10*, 428–440.

(26) Alecu, I. M.; Zheng, J.; Papajak, E.; Yu, T.; Truhlar, D. G. Biofuel Combustion. Energetics And Kinetics Of Hydrogen Abstraction From Carbon-1 In *n*-Butanol By The Hydroperoxyl Radical Calculated By Coupled Cluster And Density Functional Theories And Multistructural Variational Transition-State Theory With Multidimensional Tunneling. *J. Phys. Chem. A* **2012**, *116*, 12206–12213.

(27) Seal, P.; Papajak, E.; Truhlar, D. G. Kinetics Of The Hydrogen Abstraction From Carbon-3 Of 1-Butanol By Hydroperoxyl Radical: Multi-Structural Variational Transition-State Calcu-

lations Of A Reaction With 262 Conformations Of The Transition State. *J. Phys. Chem. Lett.* **2012**, *3*, 264–271.

(28) Katsikadakos, D.; Zhou, C.-W.; Simmie, J.; Curran, H.; Hunt, P.; Hardalupas, Y.; Taylor, A. Rate Constants Of Hydrogen Abstraction By Methyl Radical From *n*-Butanol And A Comparison Of CanTherm, MultiWell And VariFlex. *Proc. Comb. Inst.* **2013**, *34*, 483–491.

(29) Goldsmith, C. F.; Tomlin, A. S.; Klippenstein, S. J. Uncertainty Propagation In The Derivation Of Phenomenological Rate Coefficients From Theory: A Case Study Of n-Propyl Radical Oxidation. *Proc. Combust. Inst.* **2013**, *34*, 177–185.

Graphical TOC Entry